

## AN INNOVATIVE METHOD TO ENABLE STABLE, HIGH EFFICIENT, EVAPORATION IN THIN VOLUME ORC EVAPORATOR MODULES

C.M. Rops<sup>1\*</sup>, P.B.T.H. Boerboom<sup>1</sup>

<sup>1</sup>TNO Industry,  
High Tech Campus 25, 5656 AE Eindhoven, The Netherlands  
cor.rops@tno.nl

\* Corresponding Author

### ABSTRACT

Boiling explosions, due to the explosive vapour bubble growth, in small diameter/ thin volume channels are identified as the origin of flow maldistributions leading to sub-optimal thermal system performance. Insights to control the explosive growth properly are even used to employ the phenomenon to our advantage. The control over the boiling explosions has led to the elimination of the large pressure fluctuations causing the unwanted fluid backflow. Additionally the fast liquid propulsion through the evaporator is annihilated, providing enough time to fully evaporate and use the full thermal capacity of the evaporator.

Currently, the above mentioned knowledge has been used to realise numerical models describing the flow boiling heat transfer in our innovative structure. Furthermore, heat transfer models on the hot fluid side (eg. Flue gases) incorporating fin structures are developed. Combining these models, amongst others, allows us to propose evaporators based on a counterflow heat exchanger layout. Further optimisation studies show a potential vapour mass flow gain of about 25% compared to currently conventional crossflow evaporators. Additionally, the counterflow principle allows more compactness and/or significant pressure drop reductions.

### 1. INTRODUCTION

Due to the developments on Waste Heat Recovery (WHR) systems in the industry, flow boiling in thin spaces has gained attention over the last decade (Bertsch *et al.*, 2008). For example, WHR systems for heavy duty vehicles are explored and WHR opportunities for hybrid and fuel cell powered vehicles are identified as well. The elevated fluid temperatures, commonly dumped to the environment, are now used in an ORC to create a pressurised vapour which drives the expander. This expander provides mechanical or electrical energy. The more heat extracted, the more vapour mass flow created, the more energy the expander can realise (Fiaschi *et al.*, 2012). Due to the advantageous temperature profiles (Logarithmic Mean Temperature Difference) inside a counterflow heat exchanger, this type of heat exchanger is known to be most efficient (Green and Perry, 2007). However, in industry due to boiling explosions occurring in small diameter/ thin volume channels and practical header connection reasons, most evaporators employ some kind of crossflow heat exchanger layout.

Our investigations (e.g. Rops *et al.*, 2008) on boiling explosions in small diameter channels have given us understanding on the origin of the exponential vapour bubble growth. This knowledge on the proper scaling factors has led to the insights to control them properly. Furthermore, we have developed an innovative structure to use the phenomenon to our advantage (Rops *et al.*, 2009). The control over the boiling explosions allows to use two-phase flow boiling in thin volumes without the large pressure fluctuations which cause the unwanted backflow. Additionally, the fast liquid propulsion through the evaporator is annihilated. Therefore the fluid has enough time to fully evaporate and a once-through evaporation layout is possible, which is required for a proper counterflow evaporator design.

Over the last years, the analytical and experimental knowledge is brought together in numerical models. These numerical models are able to describe the flow boiling heat transfer in small diameter channels assuming the explosive vapour bubble growth is suppressed. In the section 2 the background of these models will be explained further. Likewise, the heat transfer models describing the hot fluid side (eg. Flue gases) of the evaporative heat exchanger will be discussed further. In section 3 some results of a parameter study will be given, followed by a discussion and conclusions in the final section.

## 2. NUMERICAL MODELING BACKGROUND

An evaporative heat exchanger consists of two fluid flows: one hot fluid (e.g. flue gases) from which the heat needs to be extracted, and a cool fluid (e.g. ethanol) which receives the energy and uses it to vaporise and form a (pressurised) gas, see Figure 1.

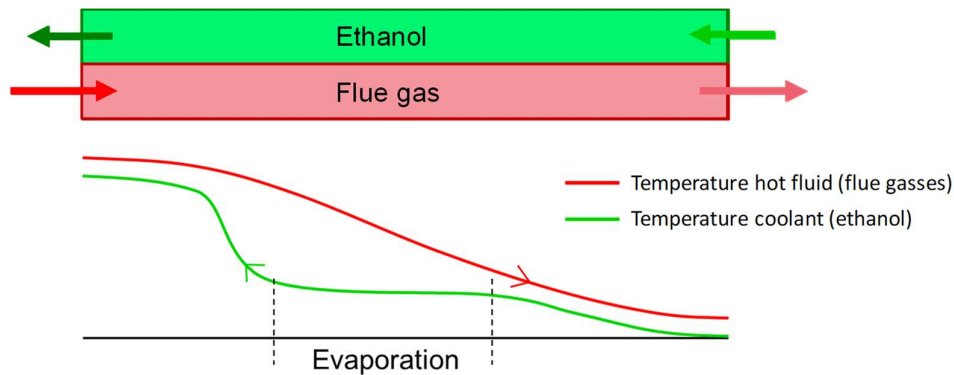


**Figure 1:** Schematic overview of a counterflow heat exchanger and indicative temperature profiles.

The schematic temperature profile for an evaporative (counterflow) heat exchanger shows that during the boiling stage the temperature of the coolant does not change significantly. Therefore the temperature difference between the hot fluid and the coolant is large, which results in a large heat flux. As long as the boiling coolant flow can absorb the heat, this is a very efficient way to extract heat out of the hot flue gases. This efficient region reduces the required surface area for heat exchange.

Since energy always flows from the higher temperature to the colder temperature, one can reason that for any heat exchanger holds that the exit temperature of the hot fluid flow,  $T_{hot\ fluid, out}$ , can not be colder than the entry temperature of the cold coolant,  $T_{coolant, in}$ . Therefore the effectiveness,  $\eta$ , of a heat exchanger can be related to this thermodynamic maximum, equation (1).

$$\eta = \frac{T_{hot\ fluid, in} - T_{hot\ fluid, out}}{T_{hot\ fluid, in} - T_{coolant, in}} \times 100\% \quad (1)$$

A conventional method like the logarithmic mean temperature difference (LMTD) approach is convenient for counter flow single phase heat transfer heat exchangers. However, due to the constant temperature section during the boiling a discretization approach is required containing appropriate heat transfer models for the various sections. The discretisation must set such (small enough) that it does not affect the solution. The heat extracted from the hot fluid can be estimated using Newton law in which the heat flow,  $q$ , is proportional to the temperature difference,  $T - T_0$ , the heat exchanging area,  $A$ , and a heat transfer coefficient,  $\alpha$ , equation (2).

$$q = \alpha \cdot A \cdot (T - T_0) \quad (2)$$

Next, a similar equation can be used to estimate the energy absorbed by the coolant. For both cases this heat extraction/absorption then affects the internal energy of the fluid flow,  $\phi$ , by cooling down or heating up in equivalent amount.

$$q = \phi \cdot c_p \cdot \Delta T \quad (3)$$

In equation (3)  $c_p$  stands for the thermal capacity and  $\Delta T$  for the fluid temperature difference between before and after the heat exchange. Equating equation (2) and (3) the temperature profile over the length of the (single phase) heat exchanger can be calculated. In case of the boiling stage the energy is no longer used to raise the temperature, but the energy is employed to overcome the latent heat,  $h_{ev}$ , and the liquid mass is converted into a vapour mass flow,  $\phi$ .

$$q = \phi \cdot h_{ev} \quad (4)$$

Therefore, in the boiling stage equation (4) needs to be equated to equation (2), while the fluid temperature remains at boiling temperature. The production of vapour changes the vapour quality and the velocity of the fluid mixture, which has an impact on both the single phase and flow boiling heat transfer coefficients. Void fraction models are applied to obtain the appropriate mixture properties and flow conditions for all applied heat transfer models.

For single phase flows, either liquid or gas, dimensionless heat transfer relations exist to estimate the heat transfer coefficient. These relations typically depend on the fluid properties and the velocity of the fluids. Also geometrical properties, such as fins, are included in the relations estimating the heat transfer coefficient. However, in case of boiling the heat transfer coefficient not only depends on the fluid mixture and flow properties but it depends on the heat flux,  $q'' = q/A$ , as well, Thome (2004).

$$\alpha_{boiling} \sim (q'')^{0.7} \quad (5)$$

Implementing equation (2) to (5) in a numerical model allows to obtain insights in design choices to optimise an evaporative heat exchanger.

### 3. RESULTS

The numerical model is used to propose evaporator designs based on a counter flow heat exchanger. The estimated accuracy of the model is 5-10%. Several parameter studies have been executed to show the impact of different design choices such as: evaporator length, fin configuration in the flue gas side and flue gas inlet temperature. In order to have a proper comparison all other parameters are kept constant, see Figure 2. The width and height of the total evaporator block is set at 250mm. The flue gas mass flow rate is 200 gram/sec at an inlet temperature of 400 °C. The ethanol inlet temperature is 70 °C at a pressure of 20bara and the exit temperature of the ethanol is must be (at least) 200 °C.

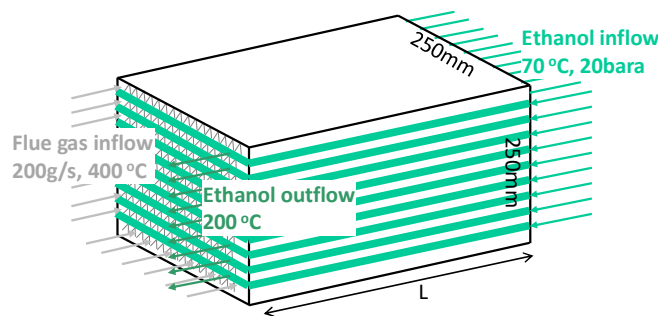


**Figure 2:** Schematic overview indicating the main parameters of the case considered.

The analysis below concerns only the evaporator, thus the possible operation of the total system (eg. expander, condenser, etc) is not included. The pressure drop over the evaporator on the ethanol side is estimated to be typically 100-300mbar for all cases. The back pressure over the flue gases is well below 10mbar for all cases. The temperature curves give an indication of the pinch point temperature difference for the various configurations.

### 3.1 Evaporator length

The first parameter to be varied is the length of the evaporator. The ethanol flow is adjusted in such a way that the exit temperature is  $\sim 215^\circ\text{C}$ .

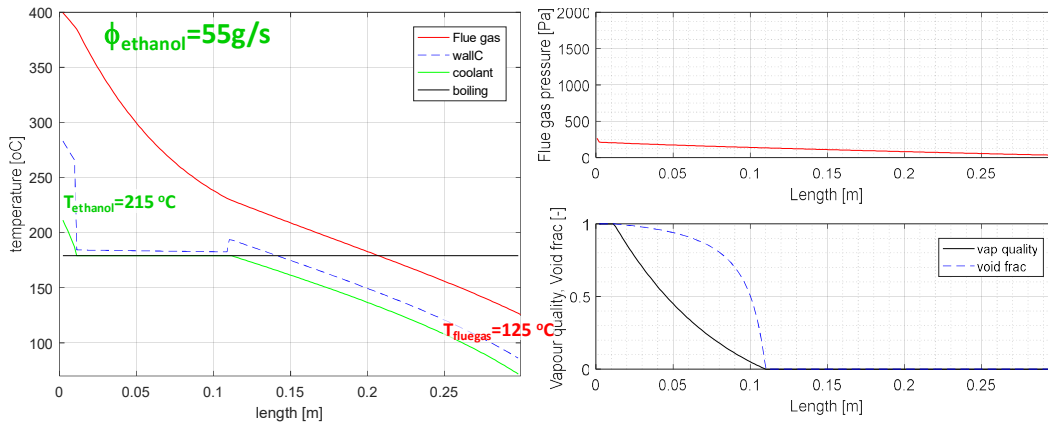


Figure 3: Typical output of the numerical model characterising the evaporator design.

Figure 3 shows some of the output of the numerical model. The estimation is that about 55g/s ethanol can be evaporated reaching the superheat requirement. The calculated temperature profiles over the length of the evaporator of the flue gases, ethanol and the wall in between are shown. In the boiling stage the wall temperature is close to the boiling ethanol temperature, which implies the high heat transfer of the boiling fluid with respect to the heat transfer from the flue gases. Furthermore, the pressure drop over the heat exchanging part of the flue gases are only a few millibar.

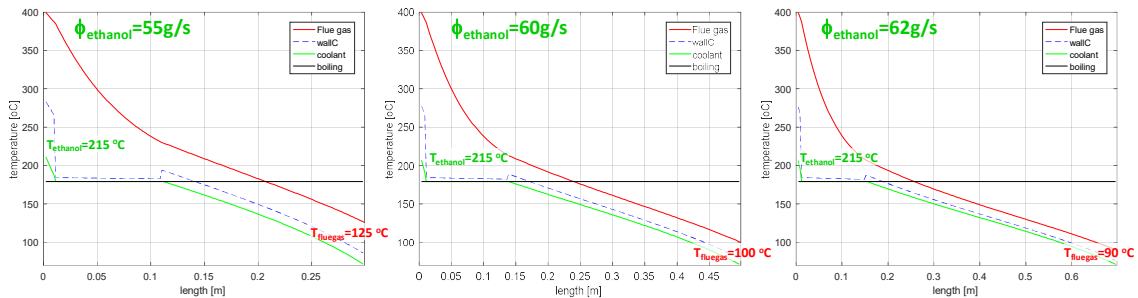


Figure 4: Effect of elongation of the evaporator.

Figure 4 shows the effect of increasing the evaporator length. Although the effectiveness,  $\eta$ , increases from 83% for a 300mm long evaporator block, 91% and 94% for a 500mm and 700mm long evaporator block, the total amount of ethanol which can be evaporated does not increase significantly on elongating the evaporator block. On the other hand, the weight of the evaporator block and the back pressure over the flue gases do increase roughly by a factor of two. Therefore, for the further parameter study a fixed length of 300mm is taken.

### 3.2 Fin configuration flue gas side

As indicated in the above paragraph, the heat transfer is limited by the heat transfer rate on the hot gas side. Optimisation of the fin structure at that side will have a positive impact on the effectiveness and the amount of ethanol which can be evaporated. In Figure 5 the effect of doubling the fin density is shown. The effect on the pressure drop is similar as the elongation of the evaporator block. However, due to the smaller temperature difference between the two fluid streams, the gain on amount of ethanol which can be evaporated is better.

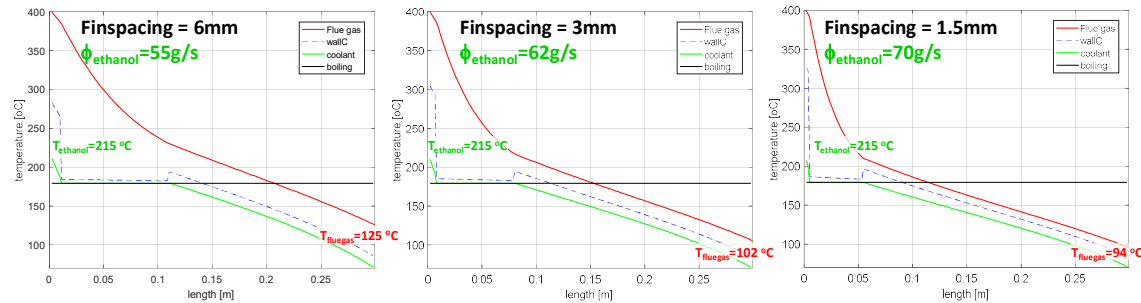


Figure 5: Effect of fin optimisation on the flue gas side.

Figure 5 shows that optimising the fin structure reduces the temperature gap between the two fluid streams. Since the boiling liquid can receive all heat, the length over which the boiling takes place is reduced. Optimisation strategy increases the maximum vapour production at the cost of little weight increase. Therefore, for the remainder of the parameter study a fixed fin spacing of 1.5mm is taken.

### 3.3 Flue gas inlet temperature

The inlet temperature of the flue gas determines to a large extent how energy is available to evaporate the ethanol. Therefore three inlet flue gas temperatures have been taken: 300 °C, 400 °C and 500 °C. The results are shown in Figure 6.

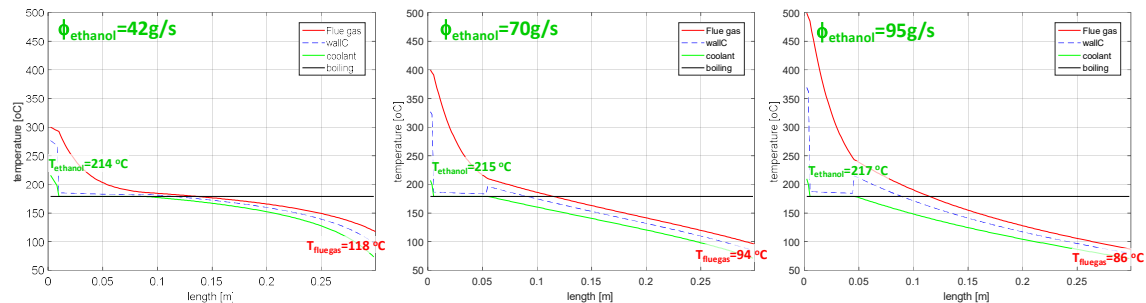


Figure 6: Effect of inlet temperature of the flue gas.

At low flue gas inlet temperature only a little amount of ethanol can be evaporated. This is due to the fact that only the amount of energy above the boiling point of ethanol (ie.  $\sim 179$  °C at 20bara) can be employed for the vapour production. Therefore, increasing the inlet temperature is beneficial over increasing the flue gas mass flow, since all the additional “temperature energy” can be employed for vapour production. While a part of the additional “mass flow” energy can not be employed for the production of vapour.

For the low inlet temperature the liquid ethanol does not contain enough energy to extract a significant amount of heat from the flue gases. This results for a relatively long length over which the temperature gap between the two streams is rather limited. This length does not contribute to the effectiveness of the evaporator. On the other hand, at high temperatures the temperature gap between the liquid ethanol

and the flue gases is widening towards the boiling stage. This shows that an optimal length can be found for specific operating points. The design of the evaporator should therefore comply to the complete range of to be expected operating points. Typical evaporator blocks currently available on the market have difficulties with the tight volume specifications, while reaching the optimal performance. Due to the counter flow mechanism, as opposed to the crossflow currently applied by the market, the potential gain in vapour production is about 25%.

#### 4. CONCLUSIONS

A numerical model based on physical heat transfer relations has been developed. A parameter study has been executed investigating the dependencies for various parameter such as the length, fin spacing and flue gas inlet temperature. The counter flow principle allows compact evaporator design, since adding additional length does not significantly improve the performance. A more suited way of increasing the vapour production is to optimise the heat transfer rate at the flue gas side, hence the fin structure. Finally, it is shown that for various operating points (different flue gas inlet temperatures) the evaporator block can be over-designed. However, the counter flow layout has a robust performance combined with its typical small volume. Therefore a stacked geometry applying a fin structure at the flue gas side and the innovative boiling structure at the coolant side allows an efficient and robust vapour production. The relatively small length needed for full evaporation results in a small back pressure for the flue gases as well.

#### NOMENCLATURE

A	area	(m <sup>2</sup> )
c <sub>p</sub>	thermal capacity	(J/kgK)
h <sub>ev</sub>	latent heat for evaporation	(J/kg)
T	temperature	(°C)
q''	heat flux	(W/m <sup>2</sup> )
q	heat flow	(W)
.		
α	heat transfer coefficient	(W/m <sup>2</sup> K)
η	effectiveness	(-)
φ	mass flow	(kg/s)

#### Subscript

coolant, in	at the entrance of the ethanol
hot fluid, in	at the entrance of the flue gases
hot fluid, out	at the exit of the flue gases

#### REFERENCES

- Bertsch S., Groll E.A., Garimella S.V., Review and Comparative Analysis of Studies on Saturated Flow Boiling in Small Channels, *CTRC Research publications, Purdue e-pubs*, 2008.
- Fiaschi D., Manfrida G., Maraschiello F., Thermo-fluid dynamics preliminary design of turbo-expanders for ORC cycles, *Applied Energy*, vol.97, pp.601–608, 2012.
- Green D.W. and Perry R.H., Perry's Chemical Engineers' Handbook, 8th edition, 2007
- Rops C.M., Geers L.F.G., Lindken R. and Westerweel J., Explosive bubble growth during flow boiling in micro channels, *5th European Thermal-Sciences Conference*, The Netherlands, 2008
- Rops C.M., Velthuis J.F.M., Graaf F., Geers L.F.G., Multiple connected channel micro evaporator, *WO2009/082230*, 2009
- Thome J.R., Wolverine engineering data book III Wolverine Tube Inc. , *Electronic distribution*, 2004.